

Geochemistry of Thermal Waters from Al-Lisi-Isbil Geothermal Field, Dhamar Governorate, Yemen

Taha Ahmed M. Al-Kohlani

Geological Survey and Minerals Resources Board, Geothermal Energy Project, P.O.Box 297, Sana'a, Yemen

tahaalkohlani@yahoo.com

Keywords: Yemen, Al-Lisi-Isbil.

ABSTRACT

The Al-Lisi – Isbil geothermal and volcanic field, one of Yemen's important fields, is known for its fumaroles, steaming grounds and hot wells. The area is mainly composed of basaltic lava flows, stratified basic tuffs and agglomerate pyroclastics. Less common are differentiated rock-types like rhyolite. The Al-Lisi volcano is an exception which consists entirely of acidic lava flows (rhyolite, obsidian, acidic tuffs and ash rings). Chemical analyses from 29 shallow water wells from the Al-Lisi – Isbil area were reviewed. All the data were interpreted using the WATCH program for speciation and by mineral equilibrium diagrams and other graphical presentation and classification methods. The maximum reservoir temperature for the wells, predicted by calculation of various geothermometers, exceeds 100°C. There is evidence of mixing with cold water. The thermal fluid is of bicarbonate type and the reservoir rocks consist mainly of sandstone (Tawilah Formation) at 1000 m to 1500 m depth.

1. INTRODUCTION

The Al-Lisi - Isbil volcanic and geothermal field is located approximately in the mid eastern part of the Dhamar governorate in central western Yemen, about 80 km south of the capital Sana'a (Figure1). Numerous boreholes for agricultural purposes have been drilled in the area and most of them contain thermal water with temperatures ranging from 21°C to 59°C, and pH values between 6.3 and 9.1. Chemical analysis have been done for the samples collected from the hot water wells, discharging from Tertiary-Quaternary igneous rocks. Temperatures and pH were measured directly in the field. Furthermore there are anomalous fumaroles (Al-Lisi) and steaming grounds (Isbil) that have low pH values (< 4.5) and TDS (< 250 ppm).

This report presents chemical data obtained from about 29 thermal and cold wells in the area. The sampling was carried out in 2007, based on the scientific collaboration between the Geological Survey and Mineral Resources Board of the Ministry of Oil, Yemen and the Department of Earth Sciences and the National Council of Research (CNR) - Study Center for Mineralgenesis and Applied Geochemistry of Florence, Italy.

The Republic of Yemen has a strategic position among the Middle East's countries. It is located on the south Arabian Peninsula, between latitudes 12 and 20° N, and between longitudes 41 and 54° E, and the total area is 527.970 km². Yemen consists of 21 Governorates. The Dhamar Governorate is in the middle of west Yemen. The AL-Lisi – Isbil volcanic area is located about 15 km east of Dhamar city. The study area is within 44°23' and 44°46' E and 14° 26' and 14° 41' N, covering approximately 740km² (Figure 1).

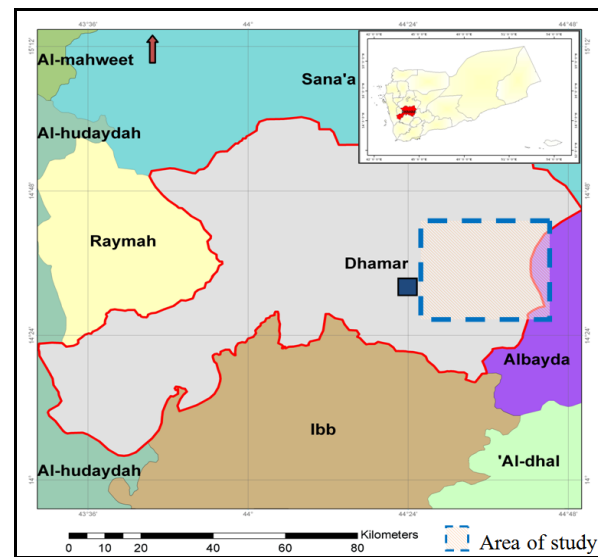


Figure 1: Location map of the Al-Lisi – Isbil area, east of Dhamar city in Yemen. The area of the present study is within the dashed box.

2. BACKGROUND AND PREVIOUS STUDIES

The western Yemen volcanic province is characterized by several hydrothermal features, such as thermal springs, condensates, fumaroles and in many cases hot water wells. These thermal features are related to relatively shallow felsic magma chambers (Mattash, 1994). The location of Yemen is thought to be one of the most active plate boundaries of the World, i.e. the triple junction made up by the Gulf of Aden, the Red Sea and the Eastern African Rift System. Alkaline flood basalts of the Yemen trap series (YTS) occupy the central-western sector of Yemen over about 50,000 km², of the age from Oligocene to Quaternary. Recent volcanic activity is present in several continental areas, such as a recent volcanic activity which occurred even in historical times near Dhamar, where a volcanic eruption was described in 1937 (Plakfer et al., 1987). Anomalous heat flow in Yemen, as a consequence of the thermal equilibrium between the upper mantle and the crust, started at 40 Ma, and reached its maximum of about 12 Ma (Elf Aquitaine, 1990 in Mattash, 1994).

The present geothermal gradient in the Red Sea region is still quite anomalous, varying from 49 to 77 °C/km, with relative heat flow ranging 94 to 154 mW/m². As a result of volcanism, anomalous heat flow and related hydrothermal circulation, relatively large epithermal alteration haloes are present in many places, such as the opalitic alteration around the Quaternary Al Lisi volcano (Mattash et al., 2001). Thermal water discharges of Yemen are highly variable in composition, due to different origin and water-rock-gas interaction processes. The majority of thermal springs and gas vents are associated with the Western

Yemen Cenozoic volcanic province. Structurally they are connected to NNW faulting parallel to the main Red Sea trend, and partially connected to Tertiary acidic intrusions. Several Quaternary to recent volcanic cones, domes craters, (such as Al-Lisi -Isbil area) and collapsed calderas are also characteristic geologic and structural features. The high-mineral contents of some thermal waters are believed to have medicinal properties (Minissale, et al., 2007).

From a classification point of view the waters of the Dhamar area have a Na (K) - Cl composition, the Al-Lisi and Isbil volcanoes is Na-HCO₃ with discharges often associated with CO₂-rich gas phase, increasing the water-rock interaction processes, that may lead to a higher degree of alteration and favoring ion-exchange reaction with Na-rich silicates, these waters thus turning to be Na-HCO₃ in composition (Mattash et al., 2001). The source of heat can be determined in some Quaternary (e.g., Dhamar-Rada'a) volcanic fields from the relatively elevated water temperatures of hot springs and also from many drilled wells, which in turn may be characteristic of geothermal reservoirs.

Equilibrium temperature evaluation of thermal reservoirs has been performed in general for Yemen using different liquid phase geothermometers, such as SiO₂, K/Mg and Na/K. Silica temperatures range between 70°C and 140°C, the highest values being calculated in Mosh Al-Kafer area. The other geothermometers display very variable values. This is particularly true for the Na/K temperatures, these values being strongly affected by mixing processes with seawater or connate waters, jeopardizing the reliability of the geothermometers (Vaselli et al., 2001).

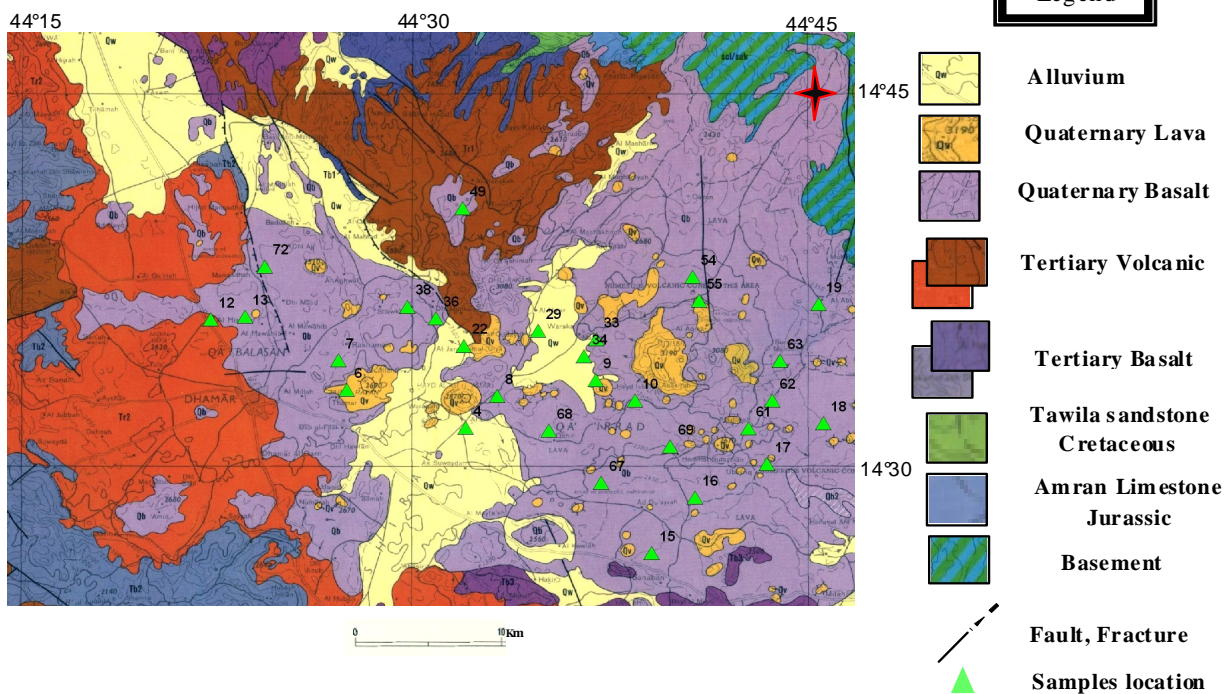


Figure 2: Geological map of study area.

3. GEOLOGY AND TECTONICS

The young volcanic series of Yemen are of the age 10-5 Ma (late Miocene to Recent) and they include eight volcanic fields with recent volcanic activities. One of them is the Dhamar-Rada'a volcanic field (Figure 3) (extensive Quaternary Volcanic) which covers an area of about 1477.1 km² and is also characterized by both central and fissure activities and has been affected by intensive vertical tectonism, resulting in the formation of horst and graben structural patterns. It is also characterized by volcanic cones, domes, sheets and lava flows. The field is mainly composed of basaltic lava flows, and lithified and stratified basic tuffs and agglomeratic pyroclastics. Less common are differentiated rock-types such as rhyolite of peralkaline character. The exception is the Al-Lisi volcano which consists entirely of acidic rocks such as rhyolite and obsidian lava flows, acidic tuffs and ash rings (Mattash et al., 2001).

The Al-Lisi-Isbil geothermal field is situated in the center of the Dhamar-Rada'a volcanic field 15 km east of Dhamar city, near the main road between Dhamar- Rada'a. The Al-Lisi volcano marks the western border of the rim; Jabal Isbil is located at the eastern rim. The latest stage of activity created the Al Lisi volcano and an explosive crater to the south. The Isbil stratovolcanic developed in the eastern study area. Several Quaternary- recent volcanic cones, craters and collapsed caldera indicate hydrothermal activity (Mattash et al., 1998).

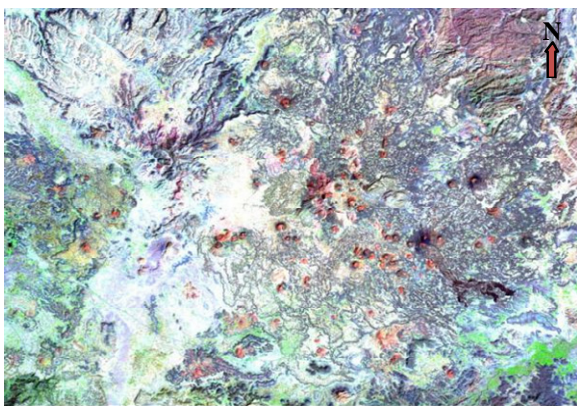


Figure 3: Landsat image, showing the Dhamar volcanic field; Location is shown in Figure 1.

Two fumaroles have been found discharging from pyroclastic deposits, mainly of obsidian volcanic glass underlying the rhyolitic lava flows. (Mattash et al., 2005). Recent fissure basaltic activity occurred throughout the whole area mainly after the terminal effusive stages of the Al-Lisi and Hammam -Isbil volcanoes. They have E-W trending fractures, which served as feeding fissures for these basalts. A structural graben that is associated with the Quaternary volcanic activity, hot springs discharging from the side of the valleys with fault direction NW-SE, parallel to the main Red Sea fault, some faults were found with NNE-SSW direction, and an E- W west direction that is parallel to the main fault, the Gulf of Aden. (Mattash and Al-Ganad, 2002).

The chronological sequence of lithological units is shown below:

- Holocene - Recent : Alluvial and wadi gravel
- Pliocene to Holocene - Quaternary : Recent volcanic
- Paleocene -Tertiary volcanic :Yemen Trap Series(YTS)
- Mesozoic - Cretaceous : Tawilah sandstone formation
- Precambrian : Basement, undifferentiated (Figure 2)

The Al-Lisi volcanic area has the following features:

- A phreatic explosion crater, south of Al-Lisi, rim is 10 m high;
- The Al-Lisi volcano with rhyolitic lava flows, explosive activity, a 330 m pyroclastic cone, surge and fall deposits, obsidian lava flow (Chiesa et al., 1983);
- Ash rings - 15 km² pyroclastic deposits, pumice and obsidian lithics;
- Lava domes - rhyolitic, peralkaline obsidian, up to 150 m high.

The Isbil volcanic complex has the following features:

- Post-caldera silicic activity, related to NNW-SSE trending fissures. 10 m surge deposits, 20 m fall deposits;
- Caldera collapse in the east part of the Isbil volcano;
- Pumice fall, 25 m thick, and pyroclastic flows;
- Isbil volcano - lava flows (3-15 m thick) with minor ignimbritic and pyroclastic deposits;
- Trachytic to rhyolitic composition, overlying Dhamar ignimbrites (Wagner et al., 2007).

3. GEOPHYSICAL STUDIES

In July 2007 a geophysical survey was carried out by a geophysical survey team of GSMRB with a German cooperation. Five vertical electrical soundings (VES) were carried out using a Schlumberger configuration of half

current spread line (AB/2) of 2000 m, to study the vertical boundaries of the aquifer system.

Four of these sites were selected by the German experts and the fifth one was executed beside a drilled well which was sealed by cement because of emission of high temperature steam during drilling.

The field data were acquired by the resistivity equipment: SYSCAL R2, automatic direct current resistivity meter, with a maximum power output of 250 Watts. The results of the geo-electrical study in the Al-Lisi area are presented in Geo-electrical cross-section in a W-E profile from sounding VES 2 to VES 4 (Figure 4). The profile has a total length of 11 km connecting 5 VES's. The cross-section illustrates the hydro-geological setting of the area.

The study indicated the existence of a conductive layer directly under the fresh water aquifer in VES 4 & 5 while they are separated by a permeable layer at VES 1, 2 & 3, this may explain the increase in water temperature of the ground water at some places, where recent studies show that the conductive layer is strongly altered rock and the geothermal layer is comprised of Tawilah sandstone. It is recommended that an exploratory borehole be drilled to a depth of 1250 m at location VES 3 to confirm the geo-electrical model and to study the geothermal aquifer.

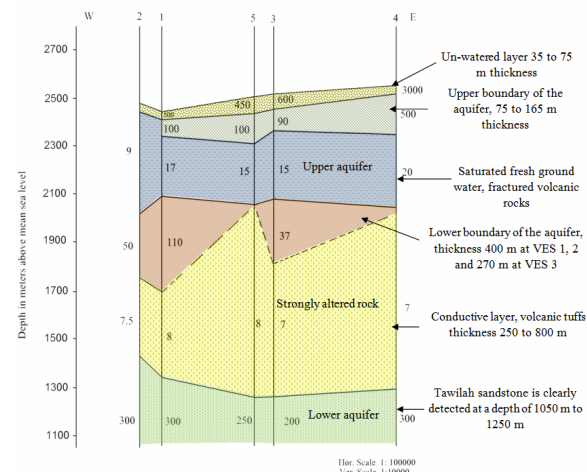


Figure 4: Geo-electrical cross-section with VES number and resistivity reading, modified after Al Shehri et al., 2007.

4. CHARACTERISTICS OF THERMAL FLUIDS

The composition of thermal fluids depends on many factors. The most important are temperature dependent reactions between host rock and fluid. Leaching also plays an important role when the amount of a particular constituent is too small to achieve equilibrium. At the same time, mixing, boiling and cooling may have considerable influence on the final composition of thermal fluids.

The wells in the Alisi- Isbil area were sampled for chemical analysis for the following elements and compounds; Ca, Mg, Na, K, HCO₃, SO₄, Cl, NO₃, B, SiO₂, F, Br, Li, and total dissolved solids (TDS) while NH₄, pH, conductivity and temperature were measured in the field. Field work was carried out by an Italian and Yemeni team in 2007 with the main focus on the north to east Dhamar province, in particular the Al-Lisi - Isbil area, after previous works and investigation had established a considerable geothermal potential in western Yemen. The samples were analyzed at the laboratories of the Department of Earth Sciences at the

University of Florence, Italy, and the CNR-Institute of Geosciences and Earth Resources in Florence.

All the solutes were determined with standard procedures using AAS (Analyst 100 Perkin Elmer), Ion Chromatography (Dionex 100) and Colorimetry (Philips Unicam). Water samples were collected from hot and cold wells as following:

1. 125 ml in a plastic bottle for the determination of anions and B; and
2. 50 ml in a plastic bottle for the determination of cations, acidified with 0.25 ml of concentrated and purified HNO_3 .

Results of chemical analysis for the samples from the 29 wells are listed in table 1. The data were plotted in different triangular classification diagrams, mixing model diagrams etc. The data were analyzed by the WATCH program for speciation and calculation of mineral equilibrium. Eight samples from eight wells were selected for the plotting of mineral saturation log (Q/K) diagrams. Linear relation between chloride content and other components was investigated.

4.1 Classification of Thermal Waters

$\text{Cl}-\text{SO}_4-\text{HCO}_3$ Triangular diagram:

The position of a data point on such a triangular plot is obtained first by summation of concentrations, C_i (mg/l), of all three constituents involved:

$$S = C_{\text{Cl}} + C_{\text{SO}_4} + C_{\text{HCO}_3} \quad (1)$$

The next step is to obtain the percent (%) of every constituent as following equations:

$$\% \text{ Cl} = 100 \text{ CCl}/S$$

$$\% \text{ SO}_4 = 100 \text{ CSO}_4/S \quad (2)$$

$$\% \text{ HCO}_3 = 100 \text{ CHCO}_3/S$$

The results of calculations for samples collected from the Al-Lisi - Isbel area are shown in Figure 5. Most of the samples are located in the high bicarbonate region or near the HCO_3 corner. Thus they can be classified as peripheral waters that may have mixed with cold groundwater or CO_2 from a magmatic source. Only three samples were located a bit closer to the chloride region of the diagram but are still within the bicarbonate water region which suggests some degree of mixing with cold water.

$\text{B}-\text{Cl}-\text{Li}$ Triangular diagram: Giggenbach (1991)

The position of a data point in such a triangular plot is simply obtained by first obtaining the sum S of the concentrations, C_i (in mg/l), of all three constituents involved:

$$S = C_{\text{Cl}}/100 + \text{CLi} + \text{CB}/4 \quad (3)$$

The next step consists of the evaluation of "% -Cl", "% -Li" and "% -B/4" according to

$$\% - \text{Cl} = 100C_{\text{Cl}}/100/S = C_{\text{Cl}}/S$$

$$\% - \text{Li} = 100C_{\text{Li}}/S \quad (4)$$

$$\% - \text{B}/4 = 100C_{\text{B}}/4/S$$

Figure (6) shows that most of the samples plot near the $\text{B} - \text{Cl}$ line, which may indicate that the fluid migrates from the young hydrothermal system, where the high absorption of B/Cl steam comes from degassing fresh magma, towards the old hydrothermal system area where there is low absorption of B/Cl steam.

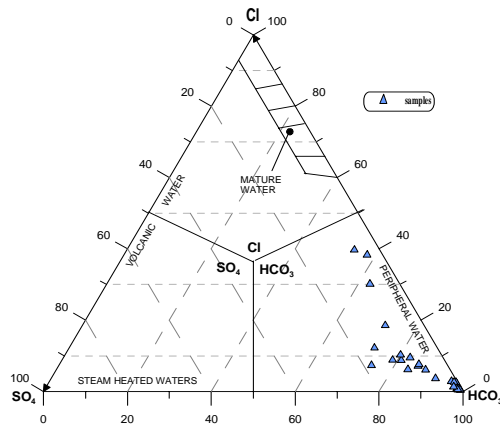
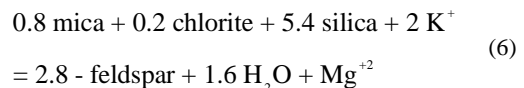
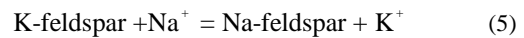


Figure 5: Classification of the AL-Lisi-Isbel wells using a $\text{Cl}-\text{SO}_4-\text{HCO}_3$ diagram.

$\text{Na}-\text{K}-\text{Mg}$ triangular diagram: The $\text{Na}-\text{K}-\text{Mg}$ diagram was constructed by Giggenbach (1988). It is essentially based on the temperature dependence of the two reactions:



The coordinates of a point on the diagram are calculated by:

$$S = C_{\text{Na}}/1000 + C_{\text{K}}/100 + \sqrt{C_{\text{Mg}}} \quad (7)$$

$$\% \text{ Na} = C_{\text{Na}}/10S$$

$$\% \text{ K} = C_{\text{K}}/S \quad (8)$$

$$\% \text{ Mg} = \sqrt{C_{\text{Mg}}}/S$$

The area of partial equilibrium suggests either a mineral that has dissolved but not attained equilibrium, or a water mixture that has reached equilibrium (e.g. geothermal water) mixed with dilute unequilibrated water (e.g. cold groundwater). Points close to the $\sqrt{\text{Mg}}$ corner usually suggest a high proportion of relatively cold groundwater, not necessarily "immature".

Figure (7) shows that almost all the samples are located in the area of immature waters, very close to the Mg corner of the diagram. This could mean they have a high proportion of cold groundwater (the reservoir fluids mix with cold groundwater) and have not attained equilibrium. The relatively high Mg concentration is due to the bicarbonate type of the water. Therefore, it is difficult to estimate reservoir temperature or not suitable. Only one sample plots between partial equilibrium and fully equilibrated water.

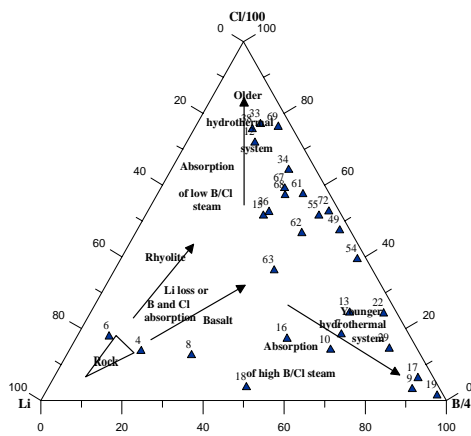


Figure 6: Classification of the thermal fluids using Li-B-Cl diagram.

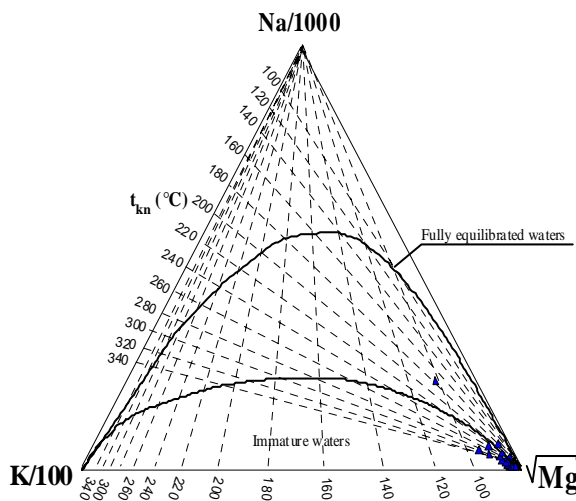


Figure 7: The Na-K-Mg diagram for thermal waters.

4.2 Geothermometers

Silica geothermometers: The dissolved concentration of silica in a hydrothermal solution can generally be used as one of the more reliable chemical geothermometer. The solubility reactions for silica minerals are invariably expressed as:



(Mineral) (silicic acid)

The silica temperature is based on the equilibrium between quartz or chalcedony and the unionized silica in a thermal fluid. Experience shows that chalcedony temperature is commonly more realistic in low temperature waters than quartz temperature (Arnórsson, 1975). Both quartz and chalcedony geothermometers were used to estimate subsurface temperatures in the present study. But there are various silica minerals with different solubilities, and it should be known which silica mineral is controlling the dissolved silica concentration when using the silica geothermometers. This means that different silica geothermometers are valid at different temperatures. Also, in mature sedimentary rocks which contain less reactive minerals, despite being a low-temperature field with temperatures less than 100°C, quartz can control dissolved silica. In another situation, chalcedony may control dissolved silica up to temperatures as high as 180°C, maybe because the chalcedony is a fine-grained variety of quartz,

which is probably not a separate mineral but a mixture of fine-grained quartz and moganite which, with time, probably all changes to quartz Gíslason et al., (1997). Therefore, there is ambiguity in the use of silica geothermometers at temperatures less than about 180°C. In general, the quartz geothermometer works well in high-temperature reservoirs, but the chalcedony geothermometer is better for low-temperature reservoirs. The reason is that at low temperatures, the rate of quartz precipitation does not cope with the rate of silica release into solution by dissolving primary minerals; on the other hand, chalcedony is unstable at temperatures above 120°C -180°C. The quartz geothermometer may be applicable down to 100°C in old systems, but in young systems, it may not be applicable below 180°C. The following equations for silica geothermometers have been proposed:

Quartz – no steam loss (Fournier, 1977):

$$T^\circ\text{C} = \frac{1309}{5.19 - \log \text{SiO}_2} - 273.15 \quad (10)$$

Quartz – maximum steam loss at 100°C (Fournier, 1977):

$$T^\circ\text{C} = \frac{1522}{5.75 - \log \text{SiO}_2} - 273.15 \quad (11)$$

Chalcedony - no steam loss (Fournier, 1977):

$$T^\circ\text{C} = \frac{1032}{4.69 - \log \text{SiO}_2} - 273.15 \quad (12)$$

Chalcedony – maximum steam loss at 100°C (Fournier, 1977):

$$T^\circ\text{C} = \frac{118}{5.09 - \log \text{SiO}_2} - 273.15 \quad (13)$$

Chalcedony - no steam loss (Arnórsson et al., 1983):

$$T^\circ\text{C} = \frac{1112}{4.91 - \log \text{SiO}_2} - 273.15 \quad (14)$$

Chalcedony – maximum steam loss at 100°C (Arnórsson et al., 1983):

$$T^\circ\text{C} = \frac{1264}{5.31 - \log \text{SiO}_2} - 273.15 \quad (15)$$

Cation geothermometers: Cation geothermometers are based on ion exchange reactions with temperature-dependent equilibrium constants. A typical example is the exchange of Na⁺ and K⁺ between co-existing alkali feldspars:



(albite) (orthoclase)

Two assumptions are made, that the activities of the solid reactions are unity and the activities of the solid reactions of the dissolved species are equal to their molal concentrations in aqueous solution. The equilibrium constant, Keq for this reaction is:

$$Keq = \frac{(\text{KAlSi}_3\text{O}_8)(\text{Na}^+)}{(\text{NaAlSi}_3\text{O}_8)(\text{K}^+)} \quad (17)$$

If the activities of the solid reactants are assumed to be unity and the activity of the dissolved species is about equal to their molal concentrations, the equation will be reduced to:

$$K_{eq} = \frac{(Na^-)}{(K^+)} \quad (18)$$

Several authors have suggested empirical Na/K geothermometers based on experiments and obtained different results due to work with different minerals. Basaltic minerals usually give low values (Arnórsson et al., 1983) but andesitic ones high values (Giggenbach, 1988) at low temperatures. At high temperatures they converge and give similar values. The Na/K ratio generally works well for estimating temperatures of water above 200°C.

The following formulae, based on empirical correlation, presented by Arnórsson et al. (1983) and Giggenbach (1988), are used in this report; the concentrations of Na and K are in mg/kg:

Na-K temperature (Arnórsson et al., 1983):

$$T^{\circ}C = \frac{933}{0.993 - \log(Na / K)} - 273.15 \quad (19)$$

Na-K temperature (Giggenbach, 1988):

$$T^{\circ}C = \frac{1390}{1.75 - \log(Na / K)} - 273.15 \quad (20)$$

K-Mg geothermometer: It is based on the equilibrium between water and the mineral assemblage K- feldspar, K-mica and chlorite (Giggenbach, 1988). It has been observed that it responds fast to changes in the physical environment and, thus, usually gives a relatively low temperature in mixed and cooled waters as compared to other geothermometers (concentrations are in mg/kg):

$$T^{\circ}C = \frac{4410}{14.4 - \log(K^2 / Mg)} - 273.15 \quad (21)$$

Na-K-Ca geothermometer: (Nicholson, 1993). The geothermometer is entirely empirical and assumes one type of base exchange reaction at temperatures above about 100°C (concentrations are in mg/kg):

$$T^{\circ}C = \frac{1647}{\log(Na / K) + \beta(\log(\sqrt{Ca / Na}) + 2.06) + 2.46} - 273.15 \quad (22)$$

Where $\beta = 4/3$ for $Ca/2Na > 1$ and $t < 100^{\circ}C$;
 $\beta = 1/3$ for $Ca/2Na < 1$ or if $t 4/3 > 100^{\circ}C$

The results of calculated geothermometers for the waters from the Al-Lisi-Isbil area are listed in Table (2)

- The K-Mg geothermometer shows values close to the measured ones.
- The silica chalcedony geothermometer gives similar values in some cases, but considerably higher in others and lower in seven cases. It is considered likely that the chalcedony geothermometer gives a minimum value for the reservoir temperatures.
- The quartz geothermometer gives considerably higher values than chalcedony and K/Mg measured in nearly all cases.
- The Na-K geothermometers indicate higher temperatures but one cannot rely on the result due to reservoir mixing

with cold waters, which makes this geothermometer unreliable. Disagreement between estimated temperatures of mentioned geothermometers might be due to mixing of samples with cold waters and thus there is no confidence to estimate reservoir temperature using this solute geothermometer.

Table 2: Temperature (°C) of different geothermometers for the thermal waters in Al-Lisi -Isbil wells.

Well no.	T meas.	T quartz ¹	T chalcedony ²	T Na-K ³	T Na-K ⁴	T K-Mg ⁴
4	29	86	55	99	154	42
6	45	75	43	75	132	51
7	30	52	20	122	173	47
8	33	80	48	145	190	47
9	36	84	52	261	279	52
10	38	86	55	289	305	56
12	28	34	3	174	212	39
13	43	37	6	202	232	44
15	35	40	9	83	139	38
16	29	94	63	176	213	57
17	37	86	55	191	224	54
18	38	47	15	225	250	66
19	28	59	27	160	201	39
22	33	76	44	167	207	37
29	40	87	56	256	275	50
33	42	90	59	250	270	58
34	43	96	65	279	296	60
36	31	78	46	148	193	31
38	35	96	65	277	294	53
49	41	47	15	94	150	95
54	32	72	40	247	290	60
55	39	60	28	211	239	56
61	38	80	49	192	225	66
62	56	100	70	220	246	79
63	59	72	40	230	255	88
67	30	70	39	130	179	58
68	35	63	31	155	199	75
69	37	81	50	247	268	63
72	21	32	1	179	215	33

(1) Fournier and potter 1982. (2) Fournier 1977.

(3) Arnorsson et al, 1983. (4) Giggenbach 1988.

4.3 Speciation and Equilibrium - the WATCH Program.

To evaluate the equilibrium minerals in the fluid, several runs of the WATCH program were done for all the wells, 49, 13, 54, 12, 15, 34, 38, 17 using the water sample analyses.

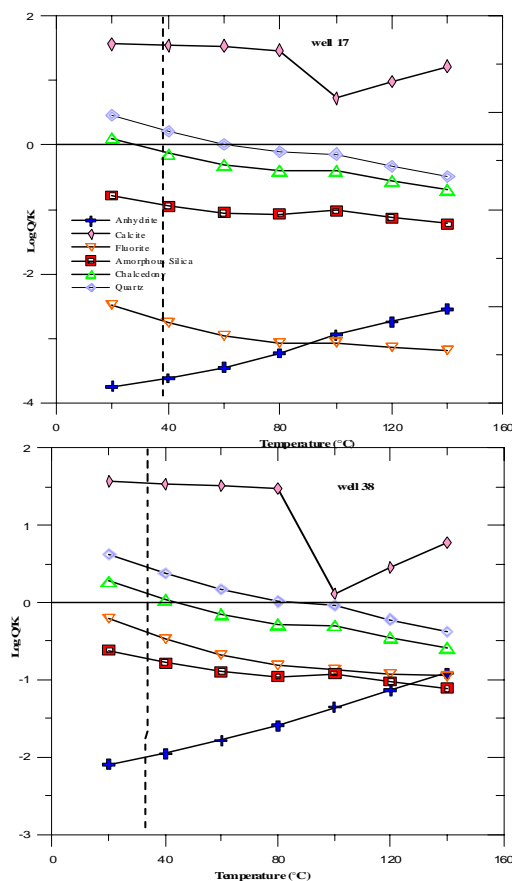


Figure 8: e.g. Saturation index (log Q/K) vs. temperature calculated with WATCH program for eight wells in the Al-Lisi – Isbil field (Dhamar area).

Figure 8 shows saturation index (SI = log Q/K) diagrams for the temperature range 20 to 140°C calculated with the WATCH aqueous speciation program which are useful to demonstrate reservoir temperatures. This method should be interpreted with caution because only three samples from wells 34, 17 and 38 have acceptable ionic balances as calculated using the WATCH program and are slightly above 10%. The following result can be obtained from the diagrams.

- Similar pattern is observed for most samples of wells and do not show any conversion to the zero saturation index by any group of minerals. It means no clear temperature-rock equilibrium is reached between all or most of the minerals and the thermal fluids can be found. This could be due to mixing or other processes such as the precipitation of some minerals.
- In almost all cases lines for two minerals cross at a temperature below the saturation line and almost all minerals plot within the undersaturation zone, which may indicate more mixing with cold groundwater.
- The pattern of the calcite saturation index plots above the zero line (supersaturated zone) in all the diagrams and furthermore, calcite solubility is inversely related to water temperature.
- Unfortunately no analysis of (Al) was available which influences the results and restricts the number of possible minerals to calculate saturation index.
- The saturation index (SI) can be applied for the evaluation of scaling potential of water. All minerals in samples are undersaturated at the calculated temperature range, except calcite. As a result, the risk of precipitation of those minerals is low.

4.4 Mixing Evaluations

Evidence of mixing: It is well known that the chemistry of geothermal water is characterized by equilibrium conditions between solutes and alteration minerals. It is also known that water formed by mixing geothermal water and cold groundwater or surface water may possess chemical characteristics too, so we can distinguish between water mixed from unmixed geothermal water. The hot rising water may show some evidence of the processes that can take place on its way to the surface; processes such as cooling by conduction, boiling or mixing with colder water, or maybe a combination of these processes. When this is the case, partial or complete chemical equilibration may or may not occur after mixing, so the chemical geothermometers indicate temperatures of the mixed water, and not the hot water within the reservoir. Hence, the temperature of the hot water cannot be estimated from a solubility relation unless the mixing is taken into account.

Geothermal waters are often, but not always, much higher in dissolved solids than cold ground and surface waters and the main chemical characteristics of mixed water, which serve to distinguish them from equilibrated geothermal waters, include relatively high concentrations of silica in relation to the discharge temperature, low pH relative to the water salinity and high total carbonate, at least if the mixing has prevented boiling.

There are numerous methods that can be used to extract some evidence about the mixing of two waters such as the relationship between chloride and boron and silica and sulfate and mixing models. The linear or near-linear relationship between these parameters appears to be useful for evaluating mixing processes and indicate that mixing has occurred. A Schoeller diagram comprises the log concentrations of fluid components from a number of analyses and shows the effects of mixing. Mixing geothermal water with dilute water moves the line on the Schoeller vertically representing an analysis without changing its shape (Truesdell, 1991).

In this study there are some indications of mixing of different water types in the studied area.

There is a disagreement between different geothermometers. Silica geothermometer temperatures are lower than the Na-K temperatures.

- The mineral equilibria diagrams show no clear intersection with the zero saturation index by any group of minerals at a particular temperature.
- In the Giggenbach Cl-SO₄-HCO₃ diagram most of the samples plot in the area for mixed water.
- In The Giggenbach Na-K-Mg triangular diagram, all the samples plot in the partially equilibrated mixed water area.
- There is a nearly linear relationship between chloride and other constituents as suggested by Arnórsson (1985) to be a good indication of mixing.
- The Schoeller diagram for samples of thermal water from the study area indicate mixing.

A semi-linear relationship between Cl vs. SO₄ and Cl vs. Na (Figure 9) is evidence that shows the ascending water might have been mixed with cold waters in upflow zone as suggested by Arnórsson (1985). There is an exception for a few scattered samples that might be waters from different origin. The same can also be said for Cl vs. SiO₂ although it is not as obvious. This is also an indication of mixing.

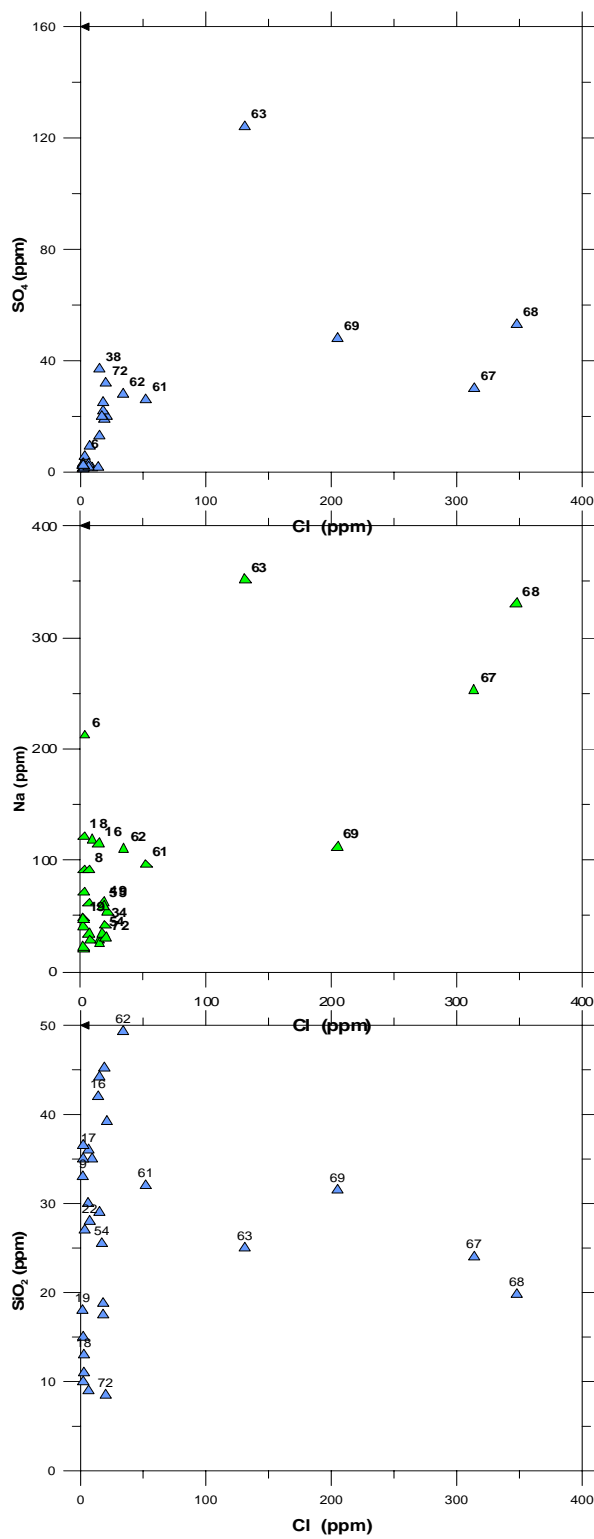


Figure 9: Relationships between Cl and SO₄, SiO₂ and Na for Al-Lisi – Isbil wells.

Schoeller diagram: This diagram is used to classify the type of water. It may be also used to show changes over time for the different water types. The effect of mixing with dilute water is to move the line representing an analysis vertically without changing its shape (Truesdell, 1991). In Figure 10, a Schoeller diagram for water from ten thermal wells and one cold well (No. 72) clearly show bicarbonate waters. As seen, there is no clear movement in connected line for some analyses to suggest mixing thermal waters with cold groundwater.

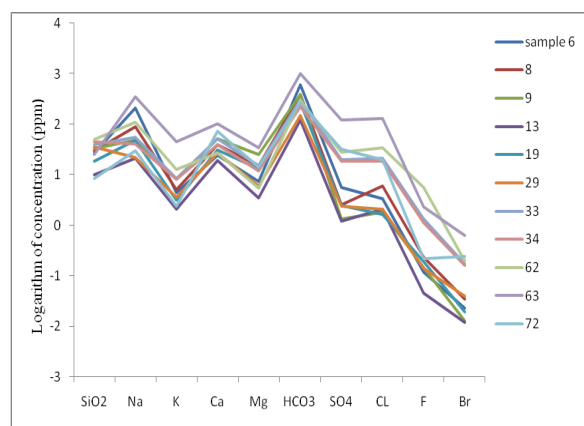


Figure 10: Schoeller diagram for Al-Lisi – Isbil wells samples.

4.5 Mixing Models

Normally the solution reactions and mineral exchange tend to re-equilibrate with cooling, but much slower at lower temperatures, so when applying mixing models to estimate subsurface temperatures, several simplifying assumptions are made. Conservation of mass and heat is always assumed, both during and after mixing. Therefore, it is assumed that chemical reactions occurring after mixing are insignificant and do not modify the water composition. Mixing models have been developed to allow for the estimation of a hot water component in mixed waters in springs or discharge from shallow drillholes. In other words when the combined heat contents of two waters at different temperatures are conserved when waters are mixed, but the combined temperatures are not, the enthalpy is used as a coordinate rather than the temperature. Under this principle, dissolved silica concentration versus enthalpy can be applied to determine the temperature of the hot water component.

Silica-enthalpy mixing model: Truesdell and Fournier (1977) proposed a simpler model that is a plot of dissolved silica versus the enthalpy of water to estimate the temperature of the deep hot water component. This model is based on the assumption that no conductive cooling occurred after mixing. If the mixed water cooled conductively after mixing, the calculated temperature of the hot water component would be too high. It is also assumed that no further silica solution and deposition occurred before or after mixing. There are some criteria for hot spring waters which may be appropriate for the application of this mode:

- A measured water temperature which is at least 50°C less than calculated silica and Na-K-Ca geothermometer temperatures;
- A silica geothermometer temperature which is lower than the Na-K-Ca temperature; and
- A mass flow rate which is high enough to allow for only a little conductive cooling.

This model cannot be used for boiling springs because heat is carried away in the steam after mixing.

The silica-enthalpy mixing model was applied to the data from the Al-Lisi – Isbil geothermal field (Figure 11). Almost all plotted samples tend to cluster at one point, very close to and above the quartz solubility line. This means these samples may not be appropriate for the estimation of the reservoir temperature. However, two lines of mixing were drawn, according to the distribution of the other data points. The upper between the cold water and the mixed thermal water intersects the chalcedony solubility curve where

enthalpy is equal to 600 kJ/kg, and corresponds to the estimated reservoir temperature, 143°C. This is higher than calculated temperature estimated using the chalcedony geothermometers. The lower (black) line intersects the quartz solubility curve where enthalpy is approximately 785 kJ/kg, which gives an estimated temperature from 120°C to 185°C. This estimated temperature range is slightly higher than that using the quartz geothermometers. A reservoir temperature of 185°C is similar to the results from the Na/K geothermometers, indicating that most of the hot waters have mixed with cooler water in the reservoir or conductive cooling probably occurs during the upflow of the hot waters.

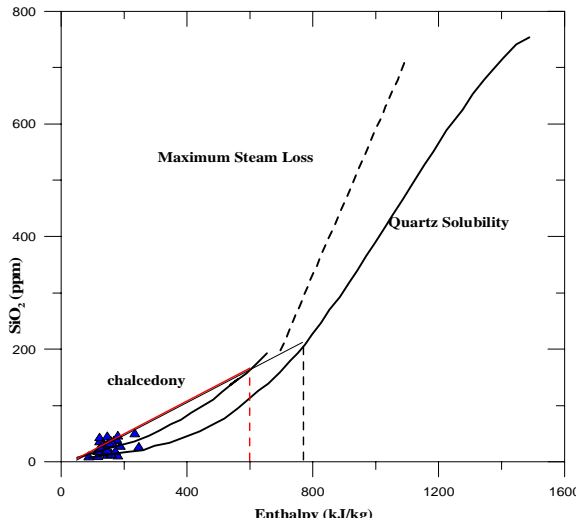


Figure 11: Silica-enthalpy mixing model for Al-Lisi - Isbil wells.

5. CONCLUSION

Exploration of geothermal sources in Yemen has been conducted since 1982 and scientific studies have been carried out since 2001 to assess the energy potential and possible use of geothermal energy for direct and indirect utilization in Yemen; until recently, these sources were only used in tourism, bathing and for irrigation purposes.



Figure 12: AL-Lisi volcanic mountain.

Water samples from 29 wells in the AL-Lisi-Isbil geothermal field were analyzed and studied using geochemical methods. The chemical composition of geothermal water in the study area is rich in Na and HCO₃ and classified as peripheral waters that may have mixed with cold groundwater or CO₂ from a magmatic source.

The Computer program WATCH 2.3 was applied for the interpretation of the chemical composition of the geothermal fluids. This program was used for the calculation of aqueous speciation, the evaluation of minerals equilibrium in the fluid and the estimation of reservoir temperature. Reservoir temperature was estimated using several geothermometers and the results were then compared. The maximum reservoir temperature was predicted to be between 100°C to 150°C in the study area.

The possibility of mixing samples with cool groundwater was evaluated by different geochemical methods such as Schoeller diagram and investigation of linear relation of chloride anion with other constituents. These methods indicate that there is evidence of mixing with cold water.

Evaluation of mineral saturation index of different minerals indicates that none of the minerals are in equilibrium. Thus no definite mineral equilibrium temperature can be observed. It also indicates that most minerals are undersaturated and the risk of precipitation is low. However, it must be noted that the calculation of equilibrium conditions was restricted due to the lack of aluminum measurements.

Exploration drilling is recommended for more detailed studies in this area to identify temperature at depth, as well as modeling, deep water sampling and the measurement of more components in water samples.

ACKNOWLEDGMENTS

I would like to express my gratitude to Dr. Ingvar B. Fridleifsson, director of the UNU Geothermal Training program and Mr. Lúdvík S. Georgsson, deputy director, for giving me the great opportunity to attend this special training and also for their generous advice and assistance. And I am grateful to the UNU-GTP staff, Ms. Thórhildur Ísberg, Ms. Dorthe H. Holm and Mr. Markus A.G. Wilde for their efficient and continuous help and kindness during the whole training. Also, my gratitude goes to Ms. Rósa S. Jónsdóttir and Ms. Guðrún Sigríður Jónsdóttir for their assistance. I wish to express my sincere gratitude to my advisor Mr. Magnús Ólafsson and Dr. Mozhgan Bagheri for their patient instruction, invaluable help and friendliness during the preparation of the report, and to Dr. Halldór Ármannsson for his support.

Grateful thanks are extended to Dr. Mohamed Ali Mattash, the head of Geothermal Energy Project, and Dr. Ismail N. Al-Ganad, general director of Geological Survey and Mineral Resources Board in Yemen for their encouraged and continued support.

I wish to give my thanks to all lecturers and staff members of ÍSOR and Orkustofnun for their comprehensive presentations and willingness to share their knowledge and experience. And finally, to my parents and my beautiful family for their emotional support and to all the 2008 UNU Fellows and MSc fellows for showing me the world, thanks.

My deepest thanks to Almighty (ALLAH) for everything.

REFERENCES

Al Shehari, K.M., and Al Hammadi, S., 2007: *Geophysical investigation of Al Lisi area - Dhamar Governorate*. Ministry of Oil and Minerals, Geological Survey and Minerals Resources Board, Yemen, unpublished report.

Arnórsson, S., 1985: *The use of mixing models and chemical geothermometers for estimating underground*

temperature in geothermal systems. *J. Volc. Geotherm. Res.*, 23, 299-335.

Arnórsson, S., Gunnlaugsson, E., and Svararsson, H., 1983: *The chemistry of geothermal waters in Iceland III. Chemical geothermometry in geothermal investigations*. *Geochim. Cosmochim. Acta*, 47, 567-577.

Arnórsson, S., 2000: *The quartz and Na/K geothermometers. I. New thermodynamic calibration*. *Proceedings of the World Geothermal Congress 2000*, Kyushu-Tohoku, Japan, 929-934.

Arnórsson, S., 1975: *Application of the silica geothermometer in low-temperature hydrothermal areas in Iceland*. *Am. J. of Sci.*, 275, 763-783.

Arnórsson, S., 1991: *Geochemistry and geothermal resources in Iceland*, In: D'Amore, F. (co-ordinator), *Applications of geochemistry in geothermal reservoir development*. UNITAR/UNDP publication, Rome, 145-196.

Arnórsson, S., 1985: *The use of mixing models and chemical geothermometers for estimating underground temperature in geothermal systems*. *J. Volc. Geotherm. Res.*, 23, 299-335.

Arnórsson, S., and Bjarnason, J.Ö., 1993: *Icelandic Water Chemistry Group presents the chemical speciation program WATCH*. Science Institute, University of Iceland, Orkustofnun, Reykjavík, 7 pp.

Bjarnason, J.Ö., 1994: *The speciation program WATCH, version 2.1*. Orkustofnun, Reykjavík, 7 pp.

Chiesa, S., Volpe, L. L., Lirer, L., and Orsi, G., 1983: *Geology of the Dhamar-Rada' volcanic field*, Yemen Arab Republic. Neues Jahrbuch fuer Geologie and Palaeontologie. Monatshefte, 481-494.

ELC, 1981: *Geology and vulcanology of the Dhamar-Rada'a region*. ELC-Electroconsult, Milan, 30 pp.

Fournier, R.O., 1977: *Chemical geothermometers and mixing model for geothermal systems*. *Geothermics*, 5, 41-50.

Fournier, R.O., and Potter, R.W. II, 1982: *A revised and expanded silica (quartz) geothermometer*. *Geoth. Res. Council Bull.*, 11-10, 3-12.

Fournier, R.O., and Truesdell, A.H., 1973: *An empirical Na-K-Ca geothermometer for natural waters*. *Geochim. Cosmochim. Acta*, 37, 1255-1275.

Giggenbach, W.F., 1988: *Geothermal solute equilibria. Derivation of Na-K-Mg-Ca geoindicators*. *Geochim. Cosmochim. Acta*, 52, 2749-2765.

Giggenbach, W.F., 1991: *Chemical techniques in geothermal exploration*. In: D'Amore, F. (co-ordinator), *Application of geochemistry in geothermal reservoir development*. UNITAR/UNDP publication, Rome, 119-142.

Gíslason, S.R., Heaney, P.J., Oelkers, E.H., and Schott, J., 1997: *Kinetic and thermodynamic properties of moganite, a novel silica polymorph*. *Geochim. Cosmochim. Acta*, 61, 1193-1204.

Mattash, M.A., Al-Ganad, I.N., As-Sarari, A.N., As-Saruri, M.A., Al-Kadasi, M.A., Muhamreq, K.M., Ba Quhaizel, M.A., Ash-Shaibani, M.S., Ash-Shami, H., Abd-Ellah, A.A., et al., 2001: *Cenozoic volcanics and geothermal potential in the republic of Yemen*. *Ministry of Oil and Mineral Resources of Yemen*, Geological Survey and Mineral Resources Board, Yemen, unpubl. report, 94 pp.

Mattash, M.A., Minissale, A., and Vasseli, O., 2005: *A proposal for exploitation of the Al-Lisi-Al Qafr-Damt geothermal prospects*. Ministry of Oil and Minerals, Geological Survey and Mineral Resources Board, Yemen, unpublished report, 32 pp.

Mattash, M.A., 1994: *Study of the Cenozoic volcanics and their associated intrusive rocks in Yemen in relation to rift development*. Univ. Budapest, Hungarian, Academy of Sciences. PhD thesis.

Mattash, M.A., Diner, J.A., and Strachan, D.G., 1998: *Epithermal alteration of the Western Yemen rift-related volcanics and their gold potential*. IMA 17th General Meeting, Toronto-Canada, Abstract volume, 123.

Mattash, M.A. and Al-Ganad, I.N., 2002: *Cenozoic volcanism and geothermal potential in the Republic of Yemen*. Ministry of Oil and Mineral Resources, Yemen, internal report, 96 pp.

Minissale, A., Mattash, M.A., Vaselli, O., Tassi, F., Al-Ganad, I.N., Selmo, E., Shawki, M.N., Tedesco, D., Poreda, R., Ad-Dukhain, A.M., et al., 2007: *Thermal springs, fumaroles and gas vents of continental Yemen: their relation with active tectonics, regional hydrology and country's geothermal potential*. *Applied Geochemistry*, 22, 799 - 820.

Nicholson, K., 1993: *Geothermal fluids: Chemistry and exploration techniques*. Springer-Verlag, Berlin, 268 pp.

Plakfer, G., Agar, R., Asker, A.H., and Haulf, M., 1987: *Surface effects and tectonic setting of the 13th December 1982 North Yemen earthquake*. *Bull. Seism. Soc. Amer.* 77, 2018-2037.

Reed, M., and Spycher, N.F., 1984: *Calculation of pH and mineral equilibria in hydrothermal waters with application to geothermometry and studies of boiling and dilution*. *Geochim. Cosmochim. Acta*, 48, 1479-1490.

Truesdell, A.H., 1991: *Effects of physical processes on geothermal fluids*. In: D'Amore, F. (coordinator), *Application of geochemistry in geothermal reservoir development*. UNITAR/UNDP publication, Rome, 71-92.

Vaselli, O., Mattash, M. A., Minissale, A., 2001: *Geothermal resources of Yemen and their geothermometric characteristics*. University of Florence, Italy, Paper No. 235-7.

Wagner, F., Mattash, M.A., and Kalberkamp, U., 2007: *Comparative reconnaissance study of three geothermal sites in Yemen*. Institute for Geosciences and Natural Resources (BGR), Germany, report, 28 pp.

Table 1: Chemical composition of geothermal waters from Al-Lisi – Isbil area in Yemen (concentration in mg/kg).

Samples	Name of wells	Longitude	Latitude	elev.	depth	T°C	pH	cond	TDS	Ca	Mg	Na	K	HCO ₃	SO ₄	Cl	NH ₄	NO ₃	B	SiO ₂	F	Br	Li
4	Al Lisi well	44 31 58	14 31 33	2460	150.00	29.0	7.01	1116	593	31.0	13.0	118	3.7	417	2	9	0.04	0.95	0.48	35.0	0.56	0.02	0.46
6	Jabel Al Dar	44 27 23	14 33 06	2415	350.00	45.0	7.00	1267	874	25.0	7.5	212	4.4	616	6	3	0.06	0.03	0.06	27.0	0.12	0.02	0.14
7	Beer Gra'yah	44 27 04	14 34 17	2407	120.00	30.0	7.94	593	400	9.0	9.0	91	3.9	282	3	2	<0.01	0.04	0.31	15.0	0.10	0.03	0.02
8	Al Makhafish	44 33 11	14 32 51	2470	160.00	33.0	7.18	963	550	40.0	15.0	91	5.1	390	3	6	<0.01	0.87	0.59	30.0	0.24	0.04	0.27
9	Al Ku'aa	44 36 58	14 33 29	2525	240.00	36.0	6.99	733	519	51.0	25.0	48	8.2	384	1	2	<0.01	1.67	2.10	33.0	0.14	0.01	0.04
10	Isbil well	44 38 28	14 32 39	2535	180.00	38.0	7.05	633	410	38.0	19.0	40	8.9	301	1	2	<0.01	1.59	0.36	35.0	0.15	0.01	0.03
12	Al-Wesabi Factory	44 22 10	14 35 55	2420	180.00	28.0	8.05	511	301	34.0	9.0	34	2.6	212	3	6	<0.01	2.82	0.06	9.0	0.05	0.03	0.01
13	Al Meshoaf	44 23 29	14 36 02	2420	200.00	43.0	7.83	344	170	19.0	3.5	21	2.1	121	1	2	0.02	1.28	0.22	10.0	0.05	0.01	<0.01
15	Sanaban	44 39 07	14 26 30	2372	240.00	35.0	7.80	427	304	7.5	4.2	71	1.7	215	2	3	<0.01	0.11	0.06	11.0	0.45	0.03	<0.01
16	Gomol	44 40 47	14 28 45	2417	150.00	29.0	6.55	1412	731	57.0	19.0	115	9.0	515	2	14	<0.01	0.91	1.70	42.0	0.18	0.04	0.25
17	Sainm	44 43 33	14 30 06	2407	280.00	37.0	7.64	700	333	17.0	9.0	61	5.5	232	2	6	<0.01	1.29	3.70	36.0	0.21	0.02	0.04
18	Al Haemedy	44 45 43	14 31 45	2378	215.00	38.0	7.02	660	691	33.0	22.0	121	15.0	495	2	3	<0.01	0.77	1.40	13.0	0.31	0.02	0.34
19	Al Abal	44 45 32	14 36 32	2280	170.00	28.0	7.49	586	361	31.0	13.0	47	3.1	263	2	2	<0.01	2.21	4.80	18.0	0.19	0.02	0.02
22	Al Mufajara	44 31 54	14 34 51	2410	146.00	33.0	7.09	367	268	34.0	6.5	28	2.0	181	9	7	0.02	5.02	0.87	28.0	1.06	0.08	0.01
29	Mufaid	44 34 45	14 35 28	2563	180.00	40.0	7.25	386	215	27.0	6.0	22	3.6	152	2	2	0.06	3.80	0.46	36.5	0.14	0.04	0.01
33	Beer Mudafer	44 36 59	14 35 08	2574	210.00	42.0	7.29	586	473	52.0	15.0	54	8.4	303	20	21	<0.01	25.00	0.17	39.2	1.30	0.17	0.02
34	Garbat Almarbou	44 36 31	14 34 26	2559	230.00	43.0	7.58	510	368	40.0	12.0	41	8.3	229	19	19	<0.01	22.00	0.34	45.2	1.14	0.16	0.02
36	Qafa Aldymah	44 30 49	14 35 58	2449	—	31.0	6.32	365	266	30.0	9.5	29	1.7	168	13	15	0.03	20.00	0.34	29.0	3.20	0.14	0.05
38	Qsm Alwatham	44 29 44	14 36 26	2434	270.00	35.0	6.86	371	275	33.0	8.2	25	5.0	152	37	15	<0.01	0.98	0.11	44.2	1.80	0.15	0.02
49	Bani Rakapan	44 31 51	14 40 24	2505	192.00	41.0	9.07	325	214	2.7	0.03	62	1.8	107	22	18	<0.01	17.00	0.76	17.5	0.32	0.31	<0.01
54	El Wathah	44 40 42	14 37 38	2485	140.00	32.5	7.77	405	268	26.0	7.2	34	6.5	157	20	17	<0.01	21.00	1.01	25.5	1.80	0.21	0.01
55	El Najd	44 40 56	14 36 40	2525	240.00	39.0	7.77	471	299	21.0	10.0	59	6.4	160	25	18	<0.01	39.00	0.60	18.8	3.40	0.24	0.02
61	El Bakalah	44 42 50	14 31 32	2500	320.00	38.5	7.91	617	414	21.0	7.6	96	8.8	203	26	52	<0.01	22.00	1.30	32.0	4.10	0.28	0.06
62	El Hornaida	44 43 45	14 32 39	2430	300.00	56.0	7.16	666	513	27.0	5.5	110	13.0	295	28	34	0.13	14.00	1.20	49.3	5.70	0.20	0.09
63	El Uglah	44 44 03	14 34 15	2370	234.00	59.0	6.48	2120	1809	102.0	35.0	352	46.0	1019	124	131	0.26	9.80	5.70	25.0	2.30	0.63	0.88
67	El Harug	44 37 11	14 29 20	2420	130.00	30.0	6.50	1760	1202	90.0	29.0	252	12.0	475	30	314	0.03	11.00	6.50	24.0	3.30	0.96	0.55
68	El Duhaimi	44 35 10	14 31 27	2490	—	34.5	6.50	1986	1316	67.0	21.0	330	21.0	476	53	348	0.01	12.00	7.70	19.8	4.50	1.20	0.68
69	El Athheel	44 39 50	14 30 49	2465	200.00	36.5	6.65	1885	968	121.0	39.0	112	17.0	426	48	205	<0.01	15.00	2.20	31.5	0.91	0.76	0.09
72	Taher	44 24 15	14 38 03	2315	150.00	21.0	7.28	923	438	72.0	14.0	30	2.4	268	32	20	0.03	11.00	0.68	8.5	0.22	0.24	<0.01